

CHROM. 16,212

## NUMERICAL ANALYSIS OF BAND DEVELOPMENT IN MULTICOMPONENT SYSTEMS FOR CHROMATOGRAPHIC SEPARATION OF ISOTOPES

TAKAO OI, HIDETAKE KAKIHANA and MAKOTO OKAMOTO\*

*Research Laboratory for Nuclear Reactors, Tokyo Institute of Technology, Ookayama, Meguro-Ku, Tokyo 152 (Japan)*

and

MASUNOBU MAEDA

*Department of Applied Chemistry, Nagoya Institute of Technology, Gokiso-cho, Showa-Ku, Nagoya 466 (Japan)*

(First received July 1st, 1983; revised manuscript received August 8th, 1983)

---

### SUMMARY

Numerical analysis of the systems closely associated with the band operation of a two-isotope chromatography was performed to show that the shapes of the isotopic mole fraction and concentration profiles were influenced by the chromatographic diffusion coefficient ratio of the two isotopes and the separation factors of the isotopes and the species responsible for the band development. These calculations yielded some interesting results, including the possibility of reverse enrichment. A mechanism is suggested that accounts for the formation of the self-sharpening boundary.

---

### INTRODUCTION

In a previous paper<sup>1</sup>, we demonstrated that the fundamental diffusion equation expressed by eqn. 1 can be applied to any kind of chromatography

$$\frac{\partial c_i(x, t)}{\partial x} = \frac{\partial}{\partial x} \left( D_i(x, t) \frac{\partial c_i(x, t)}{\partial x} \right) - \frac{\partial}{\partial x} \left( v_i(x, t) c_i(x, t) \right) \quad (1)$$

where  $c_i(x, t)$  is the concentration of species  $i$  at  $x$  (distance from the original point) and  $t$  (time),  $D_i(x, t)$  is the chromatographic diffusion coefficient of species  $i$  at  $x$  and  $t$ , and  $v_i(x, t)$  is the velocity of species  $i$  at  $x$  and  $t$ . The equation is solved mathematically, if  $D_i(x, t)$  and  $v_i(x, t)$  are assumed to be constant. On these assumptions, the solutions of eqn. 1 were derived and used to predict the influences of various factors, such as the velocity ratio and the chromatographic diffusion coefficient ratio of two isotopes and the initial bandwidth on the shapes of the isotopic mole fraction and concentration profiles in band development<sup>2</sup>. They were also applied to calculate

design and operating parameters of isotope separation equipment<sup>3,4</sup>. However, in the case of heterogeneous chromatography such as ion-exchange chromatography,  $D_i(x, t)$  and  $v_i(x, t)$  may be affected by various factors, and their constancy will rarely hold. In a heterogeneous column,  $D_i(x, t)$  and  $v_i(x, t)$  are expressed by eqns. 2 and 3, respectively<sup>5</sup>

$$D_i(x, t) \frac{\partial c_i(x, t)}{\partial x} = D_i^m(x, t) \frac{\partial}{\partial x} \left( \frac{\alpha c_i(x, t)}{\alpha + d_i} \right) + D_i^s(x, t) \frac{\partial}{\partial x} \left( \frac{d_i c_i(x, t)}{\alpha + d_i} \right) \quad (2)$$

$$v_i(x, t) = \frac{\alpha v_i^m(x, t)}{\alpha + d_i} \quad (3)$$

where  $\alpha$  is the void fraction, and superscripts m and s are for mobile and stationary phases, respectively;  $d_i$  is the distribution coefficient of species  $i$  between the mobile and stationary phases:

$$d_i = \frac{c_i^s(x, t)}{c_i^m(x, t)} (1 - \alpha) \quad (4)$$

$c_i(x, t)$  is defined by

$$c_i(x, t) = \alpha c_i^m(x, t) + (1 - \alpha) c_i^s(x, t) \quad (5)$$

As is obvious from eqns. 2 and 3,  $D_i(x, t)$  and  $v_i(x, t)$  are not essentially constant.  $D_i(x, t)$  has a particularly complex form; for some special cases it becomes simpler. If  $D_i^m(x, t)$  and  $D_i^s(x, t)$  are constant, eqn. 2 simplifies to eqn. 6

$$D_i(x, t) \frac{\partial c_i(x, t)}{\partial x} = \frac{\partial}{\partial x} \left( \frac{\alpha D_i^m + d_i D_i^s}{\alpha + d_i} c_i(x, t) \right) \quad (6)$$

If  $d_i$  is assumed to be expressed by a function of  $c_i(x, t)$  alone, in addition to the assumptions in eqn. 6, eqn. 2 reduces to eqn. 7

$$D_i(x, t) = \frac{\alpha D_i^m + d_i D_i^s}{\alpha + d_i} - \frac{\alpha(D_i^m - D_i^s)c_i(x, t)}{(\alpha + d_i)^2} \cdot \frac{dd_i}{dc_i} \quad (7)$$

As the simplest case, if  $d_i$ ,  $D_i^m$  and  $D_i^s$  are constant,  $D_i(x, t)$  has the form

$$D_i = \frac{\alpha D_i^m + d_i D_i^s}{\alpha + d_i} \quad (8)$$

This is the only case where  $D_i(x, t)$  is constant. In the case of eqns. 6 and 7, where  $D_i(x, t)$  and  $v_i(x, t)$  are not constant, it is difficult to derive mathematically the solutions of eqn. 1. In these cases numerical analysis may be employed. As was reported

in the preceding paper<sup>6</sup>, numerical calculations were carried out for the case where  $D_i(x, t)$  was expressed by eqn. 7 to show how the shape of the concentration profile in band development was influenced by the chromatographic diffusion coefficient  $D_i$ , the distribution coefficient  $d_i$ , the initial bandwidth and the flow-rate of the eluent. Because the calculations were limited to a one-component system, no information was obtained about the concentration profile of each species in a system involving more than one species or the analogue in a system involving isotopes. The reason was attributed to the fact that  $d_i$  was assumed to be provided only by the species concentration. In the case where the chromatographic diffusion coefficient is given by eqn. 6, which is more general than eqn. 7, it would be possible to obtain information about the chromatographic behaviour in systems involving more than one species or isotope.

Therefore, in the present investigation, numerical calculations based on the assumptions made in the derivation of eqn. 6 were carried out for multicomponent systems consisting of two to four different species, some of which included isotopes, so that the influences of various factors on the shapes of the concentration profile and the isotopic mole fraction profile in band development were examined.

#### ANALYSIS AND RESULTS

Besides the assumptions made in derivation of eqn. 6, the following assumptions were included in the present calculations.

(1) The total concentration of the species present in the stationary phase is constant throughout the column, *i.e.*

$$\Sigma c_i^s = c^s = \text{constant} \quad (9)$$

(2) The total concentration of the species present in the mobile phase is constant throughout the column, *i.e.*

$$\Sigma c_i^m = c^m = \text{constant} \quad (10)$$

(3) Consequently, the total concentration of the species present in both phases is constant throughout the column, *i.e.*

$$\Sigma c_i^m = c^m = \text{constant} \quad (11)$$

(4) The ratio between the distribution coefficients of two arbitrary species  $i$  and  $j$  (separation factor  $S_j^i$ ) is constant, *i.e.*

$$S_j^i = \frac{d_j}{d_i} = \text{constant} \quad (12)$$

#### *Two-component system involving species A and H*

The original concentration profiles of species A and H examined are schemat-

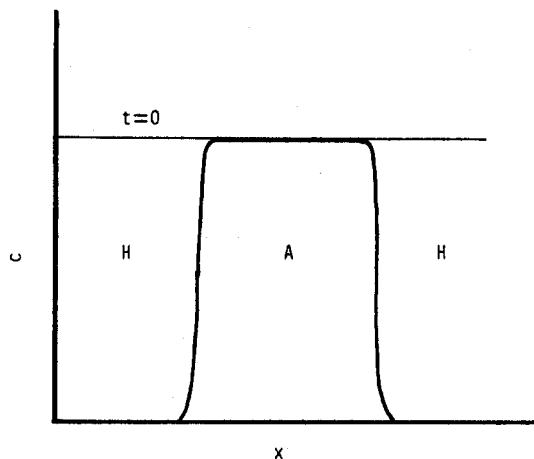


Fig. 1. Initial concentration profiles of species A and H.

ically illustrated in Fig. 1. Eqn. 10 is rewritten as eqn. 13 for the two-component system

$$c_A^m(x, t) + c_H^m(x, t) = c^m \quad (13)$$

From eqn. 11, eqn. 14 is obtained

$$c_A(x, t) + c_H(x, t) = c \quad (14)$$

$c_A^m$  and  $c_H^m$  are expressed by eqns. 15 and 16, respectively, with  $c_A$  and  $c_H$ <sup>5</sup>

$$c_A^m(x, t) = \frac{c_A(x, t)}{\alpha + d_A} \quad (15)$$

$$c_H^m(x, t) = \frac{c_H(x, t)}{\alpha + d_H} \quad (16)$$

Substitution of eqns. 12, 14, 15 and 16 into eqn. 13 leads to eqn. 17

$$\frac{c_A(x, t)}{\alpha + d_A} + \frac{c - c_A(x, t)}{\alpha + S_A^H d_A} = c^m \quad (17)$$

As is obvious from eqn. 17,  $d_A$  is given as a function of the concentration of species A only. As was described in the previous paper<sup>6</sup>, this is the case analogous to that obtained on the basis of eqn. 7, but the effect of the separation factor  $S_A^H$  on the shape of the chromatogram can be examined by means of eqn. 17. The numerical calculations were carried out as follows by use of the finite difference equation<sup>6</sup>. The

derivatives terms in eqn. 1 associated with eqns. 3 and 7 are approximated by eqns. 18, 19 and 21 with  $\Delta x$  and  $\Delta t$ , which are the small elements of  $x$  and  $t$ , respectively.

$$\frac{\partial c_i(x, t)}{\partial t} \approx \frac{c_i(x, t + \Delta t) - c_i(x, t)}{\Delta t} \quad (18)$$

$$\begin{aligned} \frac{\partial^2}{\partial x^2} \left( D_i(x, t) c_i(x, t) \right) &\approx \frac{1}{(\Delta x)^2} \{ D_i(x + \Delta x, t) c_i(x + \Delta x, t) + \\ &+ D_i(x - \Delta x, t) c_i(x - \Delta x, t) - 2D_i(x, t) c_i(x, t) \} \end{aligned} \quad (19)$$

where  $D_i(x, t)$  is defined by eqn. 20.

$$D_i(x, t) = \frac{\alpha D_i^m + d_i(x, t) D_i^s}{\alpha + d_i(x, t)} \quad (20)$$

$$\frac{\partial}{\partial x} \left( v_i(x, t) c_i(x, t) \right) \approx \frac{v_i(x + \Delta x, t) c_i(x + \Delta x, t) - v_i(x - \Delta x, t) c_i(x - \Delta x, t)}{2\Delta x} \quad (21)$$

where  $v_i(x, t)$  is defined by eqn. 3. When eqns. 18, 19 and 21 are inserted into eqn. 1, eqn. 22 is derived

$$\begin{aligned} c_i(x, t + \Delta t) &= c_i(x, t) + \\ &\frac{\Delta t}{(\Delta x)^2} \{ D_i(x + \Delta x, t) c_i(x + \Delta x, t) + D_i(x - \Delta x, t) c_i(x - \Delta x, t) - 2D_i(x, t) c_i(x, t) \} \\ &- \frac{\Delta t}{2\Delta x} \{ v_i(x + \Delta x, t) c_i(x + \Delta x, t) - v_i(x - \Delta x, t) c_i(x - \Delta x, t) \} \end{aligned} \quad (22)$$

The value of  $c_A(x, t)$  at any value of  $t$  is estimated by means of eqn. 22 according to the same procedures as in the previous work<sup>6</sup>. Because the value of  $c_A(x, 0)$  at  $t = 0$  is given as the initial condition, the  $d_A$  value at  $t = 0$  is calculated from eqn. 17.  $D_A(x, 0)$  and  $v_A(x, 0)$  and  $v_A(x, 0)$  at  $t = 0$  are then calculated with  $d_A$  according to eqn. 20 and 3, respectively. By use of these known values for  $c_A(x, 0)$ ,  $D_A(x, 0)$ ,  $D_A(x, 0)$  and  $v_A(x, 0)$ , the value for  $c_A(x, \Delta t)$  at  $t = \Delta t$  is obtained. Repetition of the above treatment gives the change of the shape of the concentration profile of species A as a function of time.

Fig. 2 shows the shapes of the concentration profiles for different  $S_A^H$  values after 20 h. It is apparent that if  $S_A^H < 1$ , the frontal part becomes sharper, whereas if  $S_A^H > 1$ , the rear part becomes sharper. It is also seen that in the case where  $S_A^H$  values are small, the chromatograms hardly migrate. This suggests that if the band

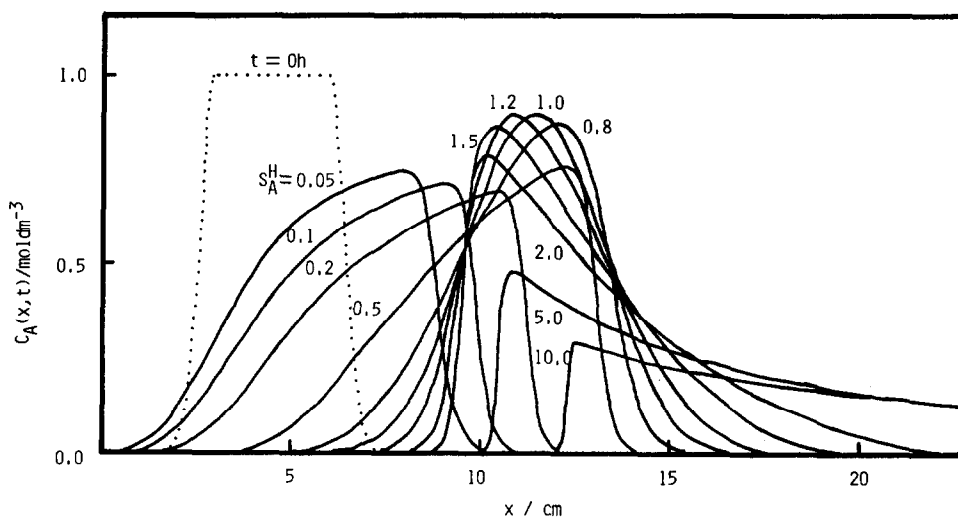


Fig. 2. Influence of  $S_A^H$  on the shape of the concentration profile;  $t = 20$  h;  $c = 1.0$  mol dm $^{-3}$ ;  $c^m = 0.0966$  mol dm $^{-3}$ ;  $D_A^s = 6.088 \cdot 10^{-6}$  cm $^2$ /sec;  $D_A^m = 1.218 \cdot 10^{-4}$  cm $^2$ /sec;  $\alpha = 0.35$ ;  $v'$  (flow-rate of eluent) = 3.6 ml/cm $^2$  h.

of A species is developed with a species H that has less affinity for the stationary phase, the band A hardly moves. In contrast, in the case of fairly large  $S_A^H$  values, the bands advance rapidly with the frontal parts flattening out more and more. This indicates that species A bypass the area of species H, which are more strongly held. These phenomena are often observed in ion-exchange chromatography. Fig. 3 shows the change of the shape of the concentration profile with increasing  $t$ .

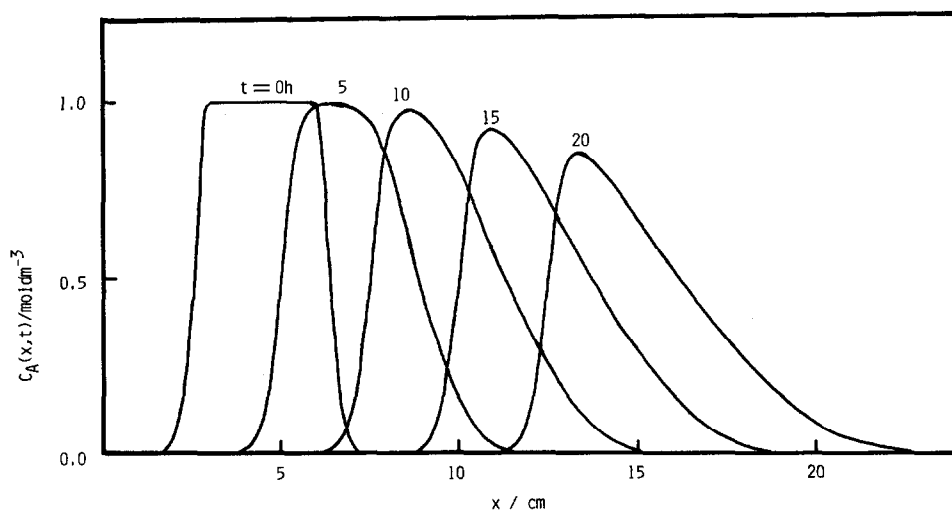


Fig. 3. Change of the concentration profile with increasing  $t$ ;  $c = 1.0$  mol dm $^{-3}$ ;  $c^m = 0.138$  mol dm $^{-3}$ ;  $D_A^s = 2.906 \cdot 10^{-6}$  cm $^2$ /sec;  $D_A^m = 1.453 \cdot 10^{-4}$  cm $^2$ /sec;  $S_A^H = 1.356$ ;  $\alpha = 0.35$ ;  $v' = 3.6$  ml/cm $^2$  h.

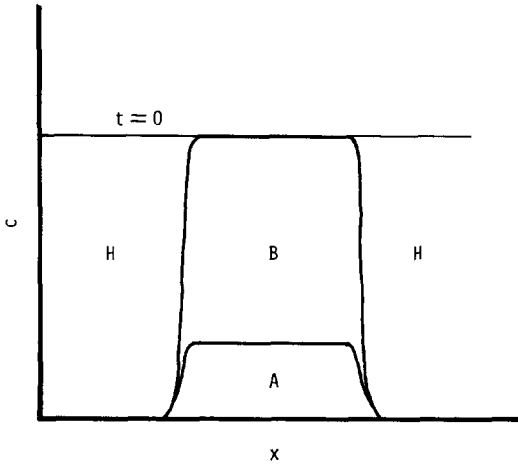


Fig. 4. Initial concentration profiles of isotopes A and B, and species H.

*Three-component system involving isotopes A and B, and species H*

The original concentration profiles of the three species examined are schematically illustrated in Fig. 4. The change of the shapes of the isotopic concentration and isotopic mole fraction profiles with increasing  $t$  was calculated for different values of  $S_A^B$ . The treatment is an obvious extension of what was described in the two-component system. Combination of eqns. 9-16 leads to eqn. 23 for  $d_A$

$$\frac{c_A(x, t)}{\alpha + d_A} + \frac{c_B(x, t)}{\alpha + S_A^B d_A} + \frac{c - c_A(x, t) - c_B(x, t)}{\alpha + S_A^H d_A} = c^m \quad (23)$$

Because the values of  $c_A(x, 0)$  and  $c_B(x, 0)$  at  $t = 0$  are given as the initial condition, the  $d_A$  value at  $t = 0$  can be calculated from eqn. 23. The  $d_B$  value at  $t = 0$  is obtained from the relationship  $d_B = S_A^B d_A$ , because  $S_A^B$  is given as a parameter value in the present case. The  $c_A(x, \Delta t)$  and  $c_B(x, \Delta t)$  values at  $t = \Delta t$  are then estimated from eqn. 22 by use of these  $d_A$  and  $d_B$  values. By repetition of these procedures,  $c_A(x, t)$ ,  $c_B(x, t)$ ,  $c_{A+B}(x, t) = c_A(x, t) + c_B(x, t)$  and  $R_A(x, t) = c_A(x, t)/c_{A+B}(x, t)$  at any  $t$  are estimated.

Fig. 5 shows the shapes of the isotopic mole fraction profile [ $R_A(x, t)$ ] and the isotopic concentration profile [ $c_{A+B}(x, t)$ ] at  $t = 20$  h for different  $S_A^B$  values.  $S_A^H$  is fixed at unity, and so the chromatograms are of the Gaussian distribution form, but they change their shapes a little with different  $S_A^B$  values (the concentration profiles are drawn for  $S_A^B = 0.9$  and  $1.1$ ). As expected, the isotope A is enriched at the frontal part when  $S_A^B > 1$ , whereas the isotope B is accumulated at the frontal part when  $S_A^B < 1$ . As the  $S_A^B$  value deviates from unity, the accumulation (depletion) curve becomes steeper.

Figs. 6 and 7 show similar plots for  $S_A^H = 0.5$  and  $2.0$ , respectively. In both cases the isotopic concentration profiles have skews analogous to those observed in the two-component system. It should be noted that the accumulation (depletion) curve on the sharper zone of the concentration profile is sharper than that on the

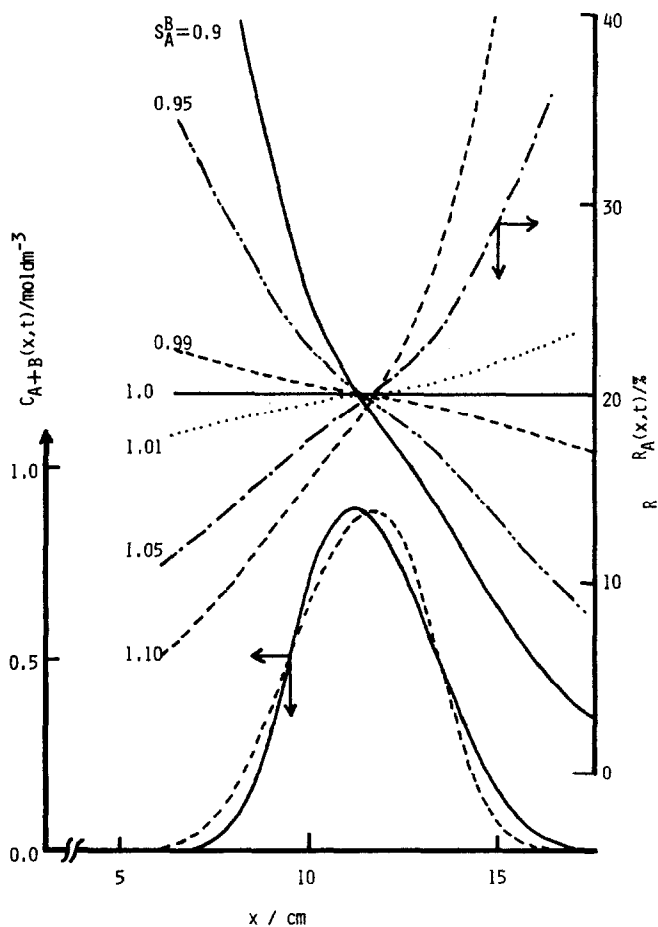


Fig. 5. Influence of  $S_A^B$  on the shapes of the isotopic mole fraction and concentration profiles;  $t = 20$  h;  $D_A^A = D_B^B = 6.088 \cdot 10^{-6}$  cm<sup>2</sup>/sec;  $D_A^B = D_B^A = 1.218 \cdot 10^{-4}$  cm<sup>2</sup>/sec;  $c = 1.0$  mol dm<sup>-3</sup>;  $c^m = 0.0966$  mol dm<sup>-3</sup>;  $\alpha = 0.35$ ;  $v' = 3.6$  ml/cm<sup>2</sup> h;  $R_A^0$  (original isotopic mole fraction) = 0.2;  $S_A^H = 1.0$ .

broader zone and that the sharper the boundary of the concentration profile is, the sharper becomes the accumulation (depletion) curve. This suggests that the experimental conditions under which the boundary of the concentration profile becomes as sharp as possible should be employed to attain as high the degree of enrichment as possible.

In Fig. 8, the isotopic mole fraction and isotopic concentration profiles were calculated for various values of the diffusion ratio of the two isotopes in mobile and stationary phases, *i.e.* for various values of  $S_B^B = D_A^m/D_B^m$  and  $S_B^s = D_A^s/D_B^s$ , with other parameters being kept constant. On changing  $S_B^B$  and  $S_B^s$  values the values of  $D_B^m$  and  $D_B^s$  were fixed. Because  $S_A^H$  is chosen to be 2.0, the concentration profiles have broad boundaries at the front and sharp ones at the rear. Even though the  $S_B^B$  and  $S_B^s$  values are changed over the range 0.9–1.1, the change of the shape of the concentration profiles is hardly discernible. Because  $S_A^B$  is taken as 1.02, the isotope



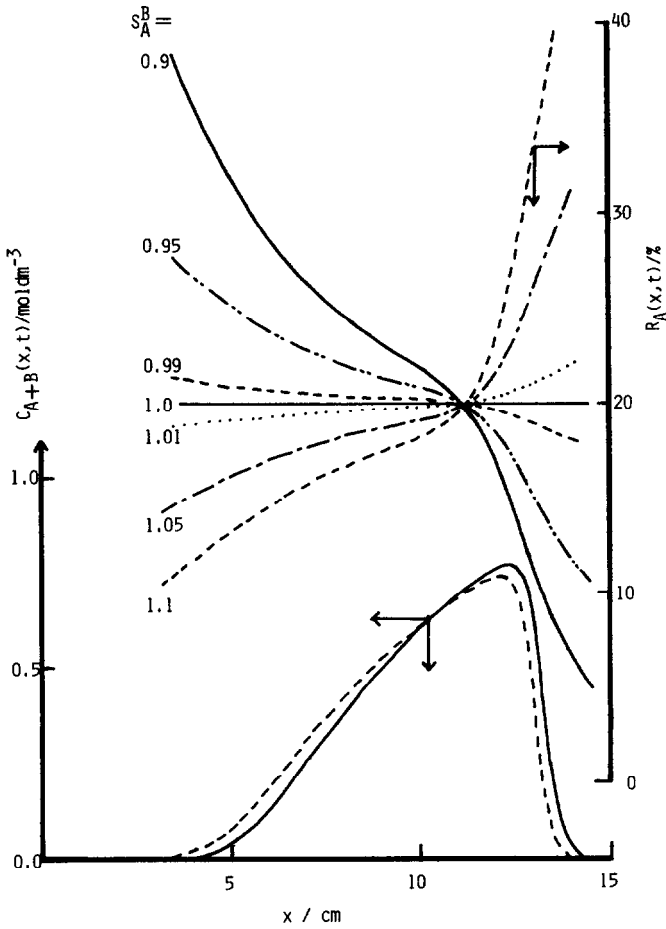


Fig. 6. Influence of  $S_A^B$  on the shapes of the isotopic mole fraction and concentration profiles;  $S_A^A = 0.5$ ; other parameter values are the same as those in Fig. 5.

A is accumulated at the frontal part and the isotope B at the rear. This trend remains unchanged even if the  $S_B^B$  and  $S_B^A$  values are varied. As the  $S_B^B$  and  $S_B^A$  values increase, the accumulation curve at the frontal part becomes sharper. In contrast, the depletion curve at the rear becomes sharper as the parameter values decrease. If the values of  $S_B^B$  and  $S_B^A$  differ substantially from unity, reverse enrichment may take place (see the curve at  $S_B^B = S_B^A = 1.1$ ).

Fig. 9 shows the change of the shapes of the isotopic mole fraction and isotopic concentration profiles with increasing  $t$ . The modes of band broadening and enrichment progress with the elapse of time are clearly seen.

*Three-component system involving three different species A, H and I*

The original concentration profiles of these species examined are schematically illustrated in Fig. 10. The application of eqns. 9-17 to the present system gives eqn. 24

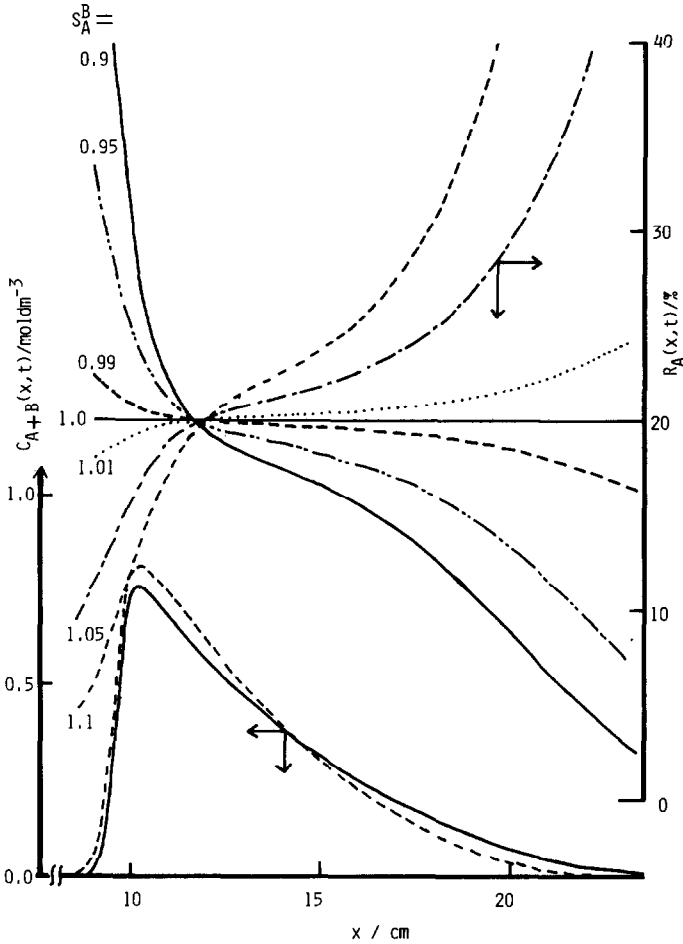


Fig. 7. Influence of  $S_A^B$  on the shapes of the isotopic mole fraction and concentration profiles;  $S_A^H = 2.0$ ; other parameter values are the same as those in Fig. 5.

$$\frac{c_A(x, t)}{\alpha + d_A} + \frac{c_H(x, t)}{\alpha + S_A^H d_A} + \frac{c - c_A(x, t) - c_H(x, t)}{\alpha + S_A^I d_A} = c^m \quad (24)$$

On the basis of eqn. 24, the influence of  $d_A$  on the shape of the concentration profile of species A was examined as follows. At the boundary between the H and A bands,  $c_A(x, t)$  is varied from 0 to  $c$ , while  $c_I(x, t) = 0$ . In this case, it is mathematically proved that  $d_A$  varies monotonically from  $c^s(1 - \alpha)/S_A^H c^m$  at  $c_A(x, t) = 0$  to  $c^s(1 - \alpha)/c^m$  at  $c_A(x, t) = c$ . At the other boundary between the A and I bands,  $d_A$  varies also monotonically from  $c^s(1 - \alpha)/S_A^I c^m$  at  $c_A(x, t) = 0$  to  $c^s(1 - \alpha)/c^m$  at  $c_A(x, t) = c$ . If  $S_A^H > 1$  and  $S_A^I < 1$ , the dependence of  $d_A$  and  $v_A$  (velocity of species A) on  $c_A$  can be calculated (Fig. 11). This figure indicates that at the frontal part the  $v_A$  value increases as the  $c_A$  value rises, whereas at the rear the  $v_A$  value decreases

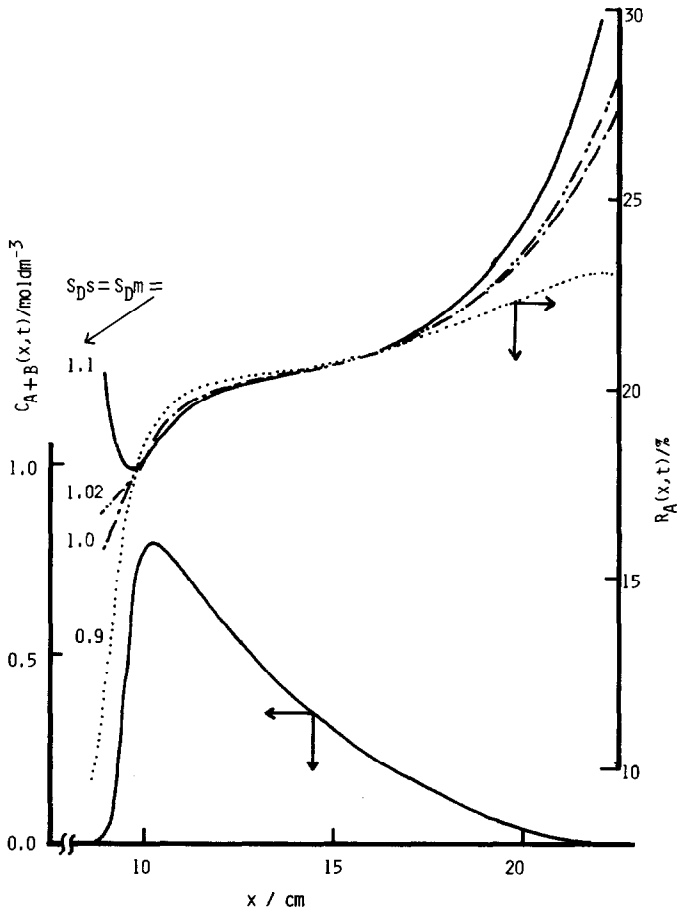


Fig. 8. Influence of  $S_D^B$  and  $S_D^A$  on the shapes of isotopic mole fraction and concentration profiles;  $S_A^H = 2.0$ ;  $S_A^B = 1.02$ ; other parameter values are the same as those in Fig. 5.

with increasing  $c_A$ . This means that if the system is chosen so that  $S_A^H > 1$  and  $S_A^I < 1$ , self-sharpening boundaries are brought about at both sides of the band A. The change of the shapes of the concentration profiles with time was calculated for different shapes of the initial bands. The calculations were carried out by means of eqns. 22 and 24 on the assumption that the system consisted of two independent two-component systems, *i.e.* H-A and A-I systems. The shapes of the boundaries were approximated by the Gauss functions, and the areas of the initial bands were kept constant. The calculated results are compared in Fig. 12 a-c. As is obvious from the figure, the chromatograms finally attain the same shape irrespective of the different shapes of the initial bands. This indicates that in the present system the driving force exists to restore distorted boundaries to self-sharpening ones. It can be said that the restoration is caused by the change of the distribution coefficient of species A or the change of the velocity of species A with the change of the species concentration.

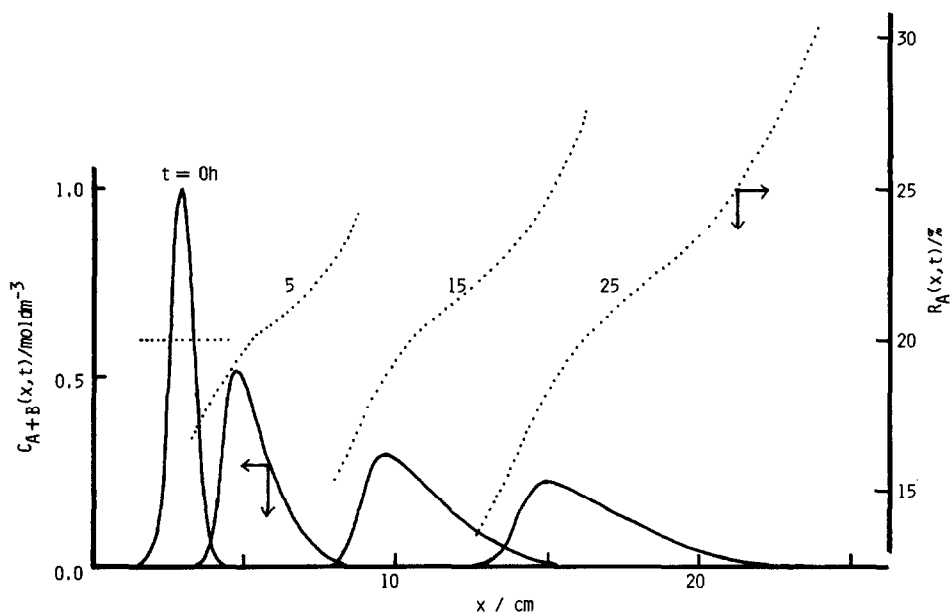


Fig. 9. Change of the isotopic mole fraction and concentration profiles with increasing  $t$ . Parameter values are the same as those in Fig. 8.

*Four-component system involving isotopes A and B, and species H and I*

The original concentration profiles of these species examined are schematically illustrated in Fig. 13. Combination of eqns. 9–16 leads to eqn. 25, which expresses the relationship between  $d_A$  and the concentrations of the relevant species.

$$\frac{c_A(x, t)}{\alpha + d_A} + \frac{c_B(x, t)}{\alpha + S_A^B d_A} + \frac{c_H(x, t)}{\alpha + S_A^H d_A} + \frac{c - c_A(x, t) - c_B(x, t) - c_H(x, t)}{\alpha + S_A^I d_A} = c^m \quad (25)$$

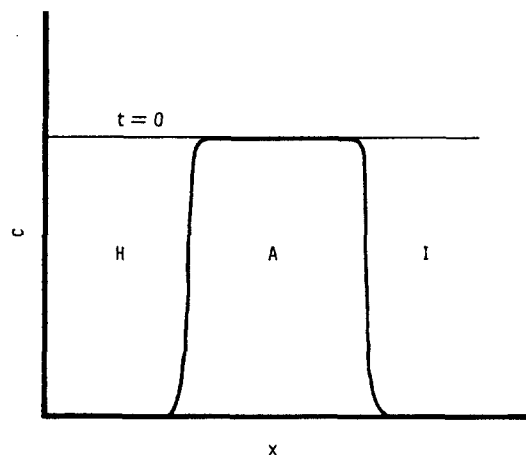


Fig. 10. Initial concentration profiles of species A, H and I.

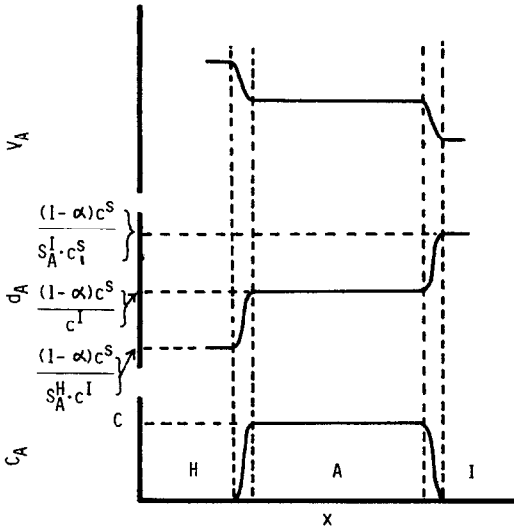


Fig. 11. Concentration dependence of  $d_A$  and  $v_A$ .

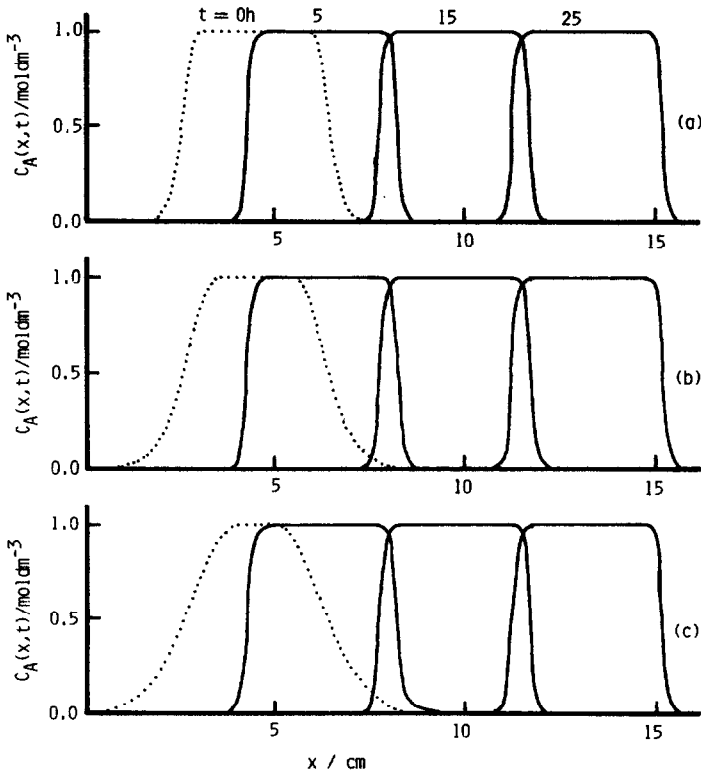


Fig. 12. Change of concentration profiles with increasing  $t$ ;  $c = 1.0 \text{ mol dm}^{-3}$ ;  $c^m = 0.0966 \text{ mol dm}^{-3}$ ;  $D_A^m = 6.088 \cdot 10^{-6} \text{ cm}^2/\text{sec}$ ;  $D_A^s = 1.218 \cdot 10^{-4} \text{ cm}^2/\text{sec}$ ;  $S_A^H = 5.0$ ;  $S_A^I = 0.2$ ;  $\alpha = 0.35$ ;  $v^I = 3.6 \text{ ml/cm}^2 \text{ h}$ .

The isotopic mole fraction and isotopic concentration profiles were calculated by means of eqns. 22 and 25 according to the same procedures as employed for the three-component system involving isotopes A and B and species H by considering that the system consisted of two independent three-component systems, *i.e.* A–B–H and A–B–I systems. The calculations were limited to the systems where self-sharpening boundaries were attained. The histories of the change of the isotopic mole fraction and concentration profiles with the elapse of time are illustrated in Fig. 14. It is seen that as the degree of enrichment proceeds, the isotopic plateau region, where  $R_A(x, t)$  equals the original isotopic mole fraction,  $R_A^0$ , gradually shrinks. In Fig. 15, the isotopic mole fraction and isotopic concentration profiles were calculated for various  $S_A^B$  values, with other parameters constant. The shape of the concentration profiles is nearly unchanged, whereas the shape of the accumulation (depletion) curves is significantly influenced by the  $S_A^B$  values. The trend of the change of the shape is the same as that observed in the three-component system involving isotopes A and B and species H.

### CONCLUSIONS

(1) In the system involving isotopes A and B, as the  $S_A^B$  value deviates from unity, the accumulation (depletion) curve becomes sharper.

(2) The shape of the accumulation (depletion) curve is more significantly influenced by the value of  $S_A^B$  than by that of  $S_D$ .

(3) If the  $S_B^B$  and  $S_D$  values deviate substantially from unity, reverse enrichment occurs.

(4) The sharper the boundary of the concentration profile is, the sharper becomes the isotopic mole fraction profile (accumulation and depletion curves). This suggests that the experimental conditions under which the boundary of the concentration profile becomes as sharp as possible should be employed to attain as high a degree of enrichment as possible.

(5) To attain the self-sharpening boundaries the species H and I which inter-

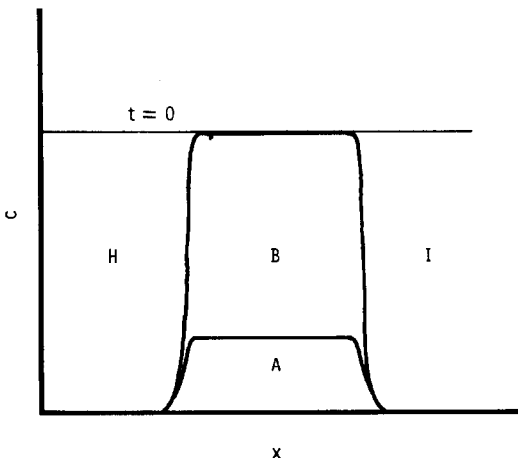


Fig. 13. Initial concentration profiles of isotopes A and B, and species H and I.

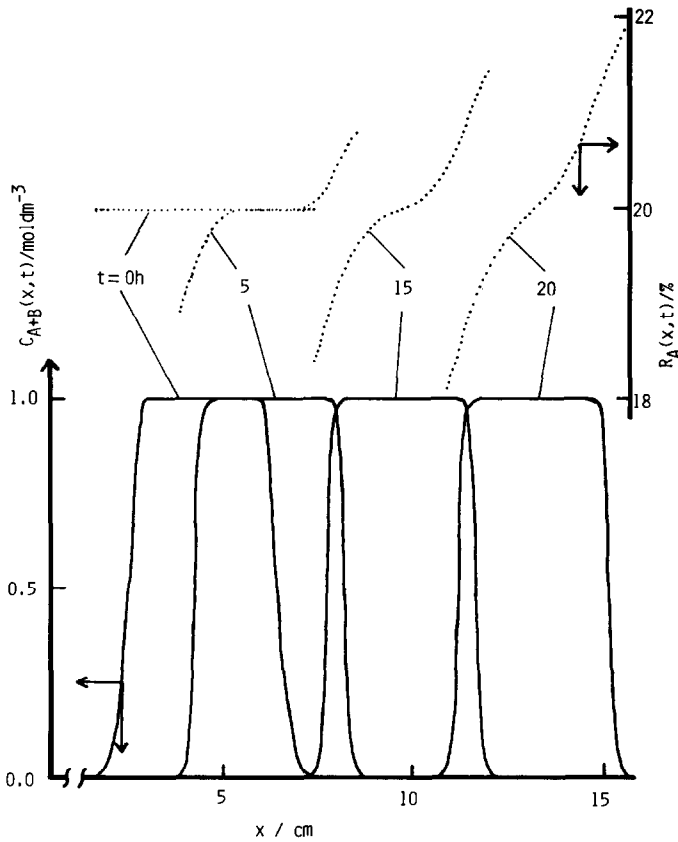


Fig. 14. Change of the isotopic mole fraction and concentration profiles with increasing  $t$ ;  $S_A^H = 5.0$ ;  $S_A^I = 0.2$ ;  $S_A^B = 1.01$ ; other parameter values are the same as those in Fig. 5.

pose the band consisting of isotopes A and B (see Fig. 13) should be chosen in such a way that  $S_A^H, S_B^H > 1$  and  $S_A^I, S_B^I < 1$ .

(6) The self-sharpening boundary is caused by the change of the distribution coefficient or the velocity of the species in question with the change of its concentration.

(7) If species H and I are chosen so that  $S_A^H, S_B^H > 1$  and  $S_A^I, S_B^I > 1$ , the frontal part of the band of A and B flattens out more and more with the elapse of time, while the rear part remains sharp. The phenomena are reversed if  $S_A^H, S_B^H < 1$  and  $S_A^I, S_B^I < 1$ .

(8) The present results are analogous to those predicted by mathematical solution on the assumption that  $D_i(x, t)$  and  $v_i(x, t)$  are constant. This suggests that the mathematical solution on the assumptions of constant  $D_i$  and  $v_i$  may be applied to the systems in which  $D_i$  and  $v_i$  are not constant in order to obtain qualitative information.

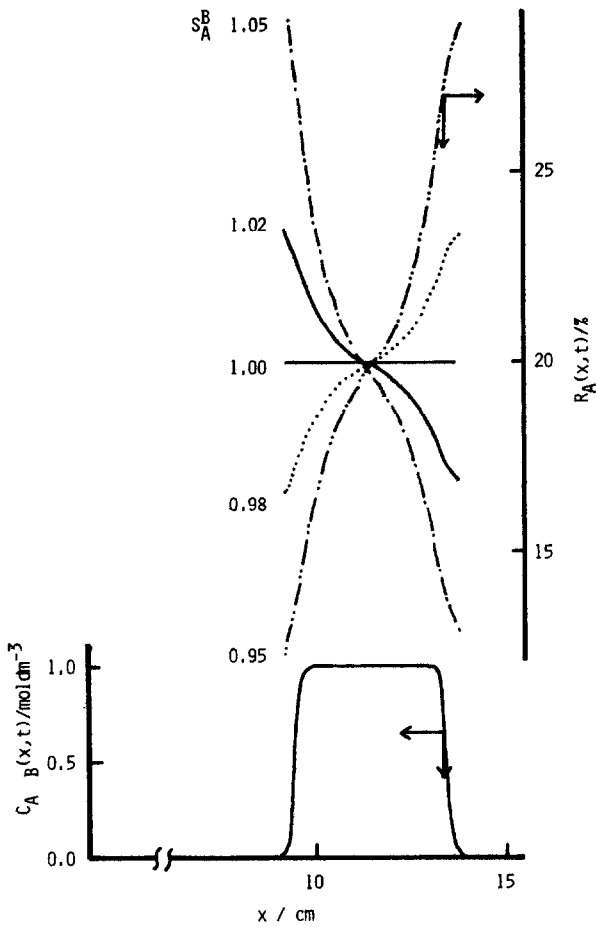


Fig. 15. Influence of  $S_A^B$  on the isotopic fraction and concentration profiles. Parameter values are the same as those in Fig. 14.

## REFERENCES

- 1 H. Kakahana, T. Oi and T. Nomura, *J. Nucl. Sci. Technol.*, 14 (1977) 572.
- 2 T. Oi, H. Kakahana and T. Nomura, *J. Nucl. Sci. Technol.*, 15 (1978) 835.
- 3 H. Kakahana, D. R. Dickeson, T. Oi and T. Nomura, *J. Nucl. Sci. Technol.*, 15 (1978) 272.
- 4 A. Nakagawa, Y. Sakuma, M. Okamoto and M. Maeda, *J. Chromatogr.*, 256 (1983) 231.
- 5 T. Oi and H. Kakahana, *J. Nucl. Sci. Technol.*, 15 (1978) 941.
- 6 T. Oi, H. Kakahana, M. Okamoto and M. Maeda, *J. Chromatogr.*, 270 (1983) 7.